Stability of Tubular Structures Based on β-Helical Proteins: Self-Assembled versus Polymerized Nanoconstructs and Wild-Type versus Mutated Sequences

David Zanuy,*,† Francisco Rodríguez-Ropero,† Nurit Haspel,‡ Jie Zheng,§ Ruth Nussinov,§,|| and Carlos Alemán*,†

Departament d'Enginyeria Química, E. T. S. d'Enginyeria Industrial de Barcelona, Universitat Politècnica de Catalunya, Diagonal 647, Barcelona E-08028, Spain, Rice University, P.O. Box 1892, Houston, Texas 77251-1892, Basic Research Program, SAIC-Frederick Inc., Center for Cancer Research, Nanobiology Program, NCI-FCRDC, Frederick, Maryland 21702, and Sackler Institute of Molecular Medicine, Department of Human Genetics and Molecular Medicine, Sackler School of Medicine, Tel Aviv University, Tel Aviv 69978, Israel

Received May 21, 2007; Revised Manuscript Received July 30, 2007

In this work we used atomistic molecular dynamics simulations to examine different aspects of tubular nanostructures constructed using protein building blocks with a β-helical conformation. Initially, we considered two different natural protein building blocks, which were extracted from the protein data base, to compare the relative stabilities of the nanotubes obtained made of self-assembled and covalently linked repeats. Results show nanotubes constructed by linking building blocks through covalent bonds are very stable suggesting that the basic principles of polymer physics are valid when the repeating units are made of large fragments of proteins. In contrast, the stability of self-assembled nanostructures strongly depends on the attractive nonbonding interactions associated to building blocks aligned in a complementary manner. On the other hand, we investigated the ability of a conformationally constrained synthetic amino acid to enhance the stability of both self-assembled and polymerized nanotubes when it is used to substitute natural residues. Specifically, we considered 1-aminocyclopentane-1-caboxylic acid, which involves strong stereochemical constraints produced by the cyclopentane side chain. We found that the incorporation of this amino acid within the more flexible regions of the β-helical building blocks is an excellent strategy to enhance the stability of the nanotubes. Thus, when a single mutation is performed in the loop region of the β-helix, the bend architecture of the whole loop is stabilized since the conformational mobility is reduced not only at the mutated position but also at the adjacent positions.

Introduction

Complex multimolecular structures can be usefully designed from biological macromolecules[1,2] via noncovalently self-assembled "foldamer" building blocks.[3] Self-assembly of peptides and proteins[4−12] and DNA[13,14] and RNA segments[15] into novel nanostructures has been reported. In these nanostructures, especially in those derived from proteins, it was proposed that suitable building blocks are composed by fragments able to retain in solution a conformation similar to that observed in the native protein structure.[11,12] Thus, manipulation of such preexisting protein foldamers may provide stable nanostructures through a favorable association process.[16−18]

Previously, we have used computer simulation methods to design tubular nanostructures based on β-helical proteins.[19] We selected 17 building blocks from native left-handed β-helical proteins by slicing β-helices into two-turn repeat units. Four copies of each structural unit were stacked one atop the other, with no covalent linkage between them. The stability of these self-assembled tube organizations was investigated through relatively short (20−40 ns) molecular dynamics (MD) simulations. Constructs which preserve their organization in the simulation are candidates for experiments. We observed that a structural model based on the self-assembly of a two-turn repeat motif from *E. coli* galactoside acetyltransferase (PDB code 1krr, chain A) produced a very stable tube. Mutational studies revealed that the stability of the self-assembly is enhanced when the mobility in the loop regions is reduced or unfavorable electrostatic interactions are eliminated.[19−21] In addition, technological applications as the formation of nanofibers to transfer charge through p-electron stacking or through H^+ transfer have been proposed.[22]

Here, our goal is to design through atomistic computer simulations a stable tubular structure using naturally occurring repeat building blocks. Current techniques do not allow simulations of the self-assembly processes. However, the systematic use of MD to screen potential assembly arrangements has proven to be an efficient and reliable tool to predict the ultrastructure of amyloid fibrils by discarding unfavorable association modes in small model systems.[23−26] In the present work, we study the stability of self-assembled versus covalently linked repeats. Regan and co-workers have recently shown that copies of structural units covalently linked by spacers lead to stable supramolecular structures.[16,18] Accordingly, we investigate if this strategy can be extended to tubular nanostructures based on polymerized β-helical repeats using MD simulations. In addition, we examine the ability of a given conformationally

* To whom correspondence should be addressed. E-mail: david.zanuy@upc.es; carlos.aleman@upc.edu.
† Universitat Politècnica de Catalunya.
‡ Rice University.
§ NCI-FCRDC.
|| Tel Aviv University.

10.1021/bm700561t CCC: $37.00 © 2007 American Chemical Society
Published on Web 09/14/2007

Table 1. Sequences of the Wild Type 1krr and 1hv9 Building Blocks Used to Construct the Nanotubes[a]

PDB	protein name	residues	sequence
1krr	galactoside acetyltransferase from e. coli	131−165	PITIGNNVWIGSHVVIN***P*** **G**VTIGDNSVIG***A***GSIVT
1hv9	*N*-acetylglucosamine 1−phosphate uridyltransferase GlmU, C−terminal domain from e. coli.	296−329	CVIKNSVIG***DD***CEISPY TVVEDANLA**A**ACTIGPF

[a] For each fragment the mutated residues are highlighted with both bolding and italics.

Table 2. Details of the Simulated Systems[a] Studied in This Work: Total Number of Particles (N_{atoms}), Number of Solvent Molecules (N_{Water}), Number of Sodium Atoms (N_{Na+}), and Size of the Simulation Box at the Beginning of the Simulation

system	N_{atoms}	N_{Water}	N_{Na+}	initial box size(Å)	simulation conditions
nanotubes					
self−assembed 1krr	56238	18040	4	80 × 80 × 110	NPT 298K NVT 350K
self−assembled 1hv9	56084	18032	16	80 × 80 × 110	NPT 298K NVT 350K
polymerized 1krr	56226	18041	4	80 × 80 × 110	NPT 298K NVT 350K
polymerized 1hv9	56129	18059	16	80 × 80 × 110	NPT 298K NVT 350K
building blocks					
1krr	17474	5656	1	56 × 56 × 56	NPT 298K
1hv9	17465	5656	4	56 × 56 × 56	NPT 298K

[a] Mutated systems in which proteogenic residues have been replaced by Ac_5c have not been explicitly specified since the variation in number of particles with respect to the wild-type system is very small.

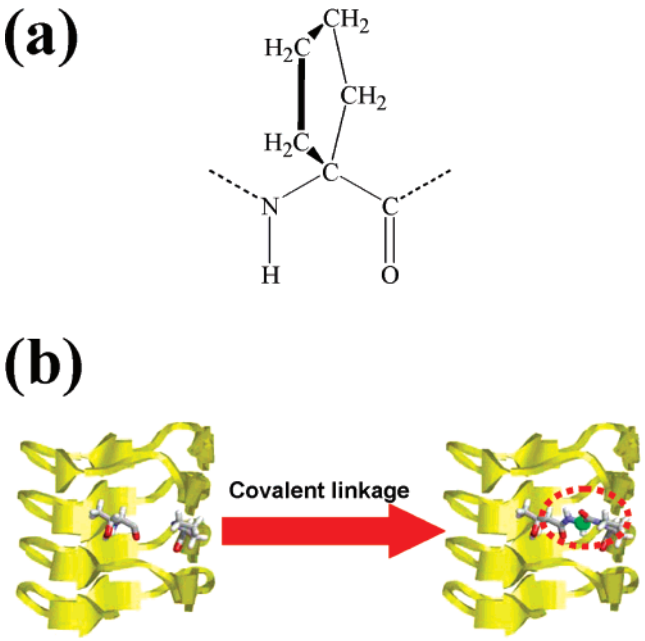

Figure 1. (a) Chemical structure of the Ac_5c residue. (b) Formation of a covalent link between two building blocks of 1krr. The Gly residue used as linker between the two building blocks is specifically displayed.

restricted synthetic residue to enhance the stability of the nanotubular construct. Specifically, we focused on 1-aminocyclopentane-1-carboxylic acid (Ac_5c), a simple cyclic α,α-dialkylated amino acid with strong stereochemical constraints induced by the cyclopentane ring (Figure 1a). A distinct structural feature of Ac_5c is that the backbone dihedral angles φ,ψ are not as geometrically restricted by the five-membered cycle as in Proline, even though the steric interactions produced by this bulky side group constrain its conformational flexibility.[27] Taking into account that the stability of the nanotubular construct is enhanced by the incorporation of proline in the loop region,[19] we decided to analyze if Ac_5c is a good candidate to increase the stability of both the repeats and the tubes formed by self-assembling and by polymerization.

On the other hand, incorporation of synthetic residues into naturally occurring building blocks may also increase resistance toward in vivo proteolysis, due to the low selectivity of proteolytic enzymes with respect to the newly incorporated amino acids, while at the same time, the presence of new functional groups may also redesign their biological function.[28,29]

Description of the β-Helical Building Blocks and the Ac_5c Synthetic Residue. Previously,[19] left-handed β-helical building blocks were selected for nanotubular structural design according to the following criteria: (i) they contain highly repetitive, symmetrical building blocks allowing formation of nanofibers without performing many structural manipulations;[16] (ii) they mostly occur in or near active or binding sites, thus likely to be of functional importance;[30−36] and (iii) as compared with right-handed β-helices, left-handed β-helices exhibit small variability of shape, size, and sequence.[37] Left-handed β-helices display an equilateral triangular shape and highly repetitive sequence, whereas right-handed β-helices are less regular. We found that a nanotube constructed of four stacked replicas of the left-handed β-helix formed by residues 131−165 of 1krr exhibited remarkable stability under different simulated conditions, including temperature increase and addition of ions.[19] On the other hand, the less stable model was obtained from four self-assembled copies of the β-helix formed by residues 296−329 of *N*-acetylglucosamine-1-phosphate uridyltransferase GlmU, C-terminal domain from *E. coli* (PDB code 1hv9). Thus, nanoconstructs formed by this repeat are good systems to test stabilization strategies, and models constructed from both 1krr and 1hv9 have been used to compare the stability of the nanotubes produced by self-assembly versus covalent polymerization. A description of the sequences used to create the models based on 1krr and 1hv9 repeats is provided in Table 1. Each sequence contains a repetitive helical strand-loop motif, where the peptide backbones alternate between β-strands and loops. X-ray crystal structures of both 1krr and 1hv9 show that these two protein fragments have an almost perfect equilateral triangular shape, with each side being ∼18 Å.

Studies of peptides containing the Ac_5c residue have indicated that this synthetic amino acid presents a restricted conformational space with a high propensity to adopt folded conformations.[27,38,39] This conformational characteristic makes Ac_5c a potential candidate to reduce the conformational freedom of the β-helix building blocks if it is introduced in the most mobile regions, i.e., the folded loops, replacing natural amino acids. Furthermore, the strain energy associated with the cyclopentane ring in Ac_5c is significantly lower than that of other constrained

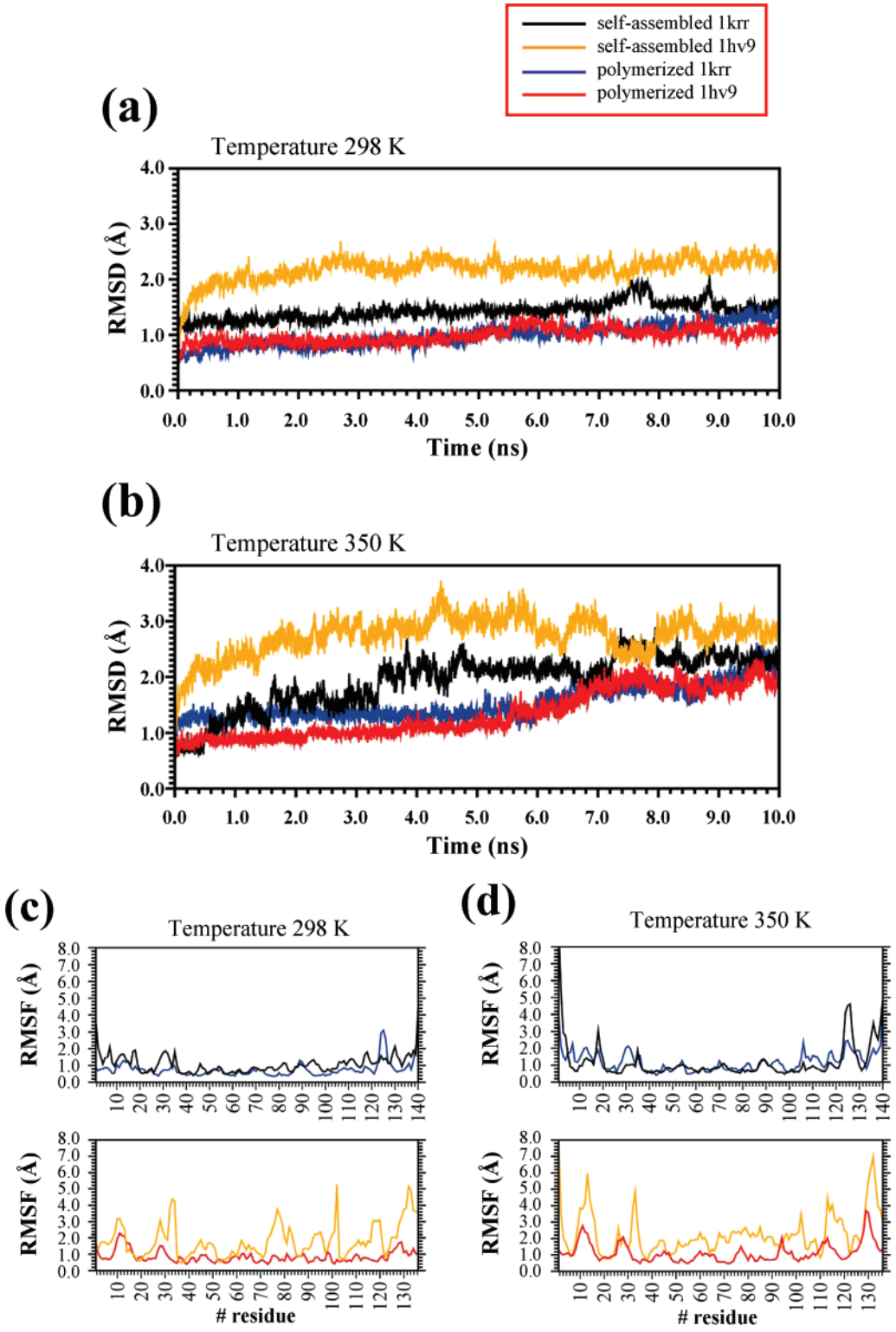

Figure 2. Evolution of the backbone RMSD of the simulated wild type nanotube models with respect to the initial structure at 298 (a) and 350 K (b): self-assembled 1krr (black), self-assembled 1hv9 (orange), polymerized 1krr (blue) and polymerized 1hv9 (red). (c) RMSF of the 1krr (top) and 1hv9 (bottom) polymerized nanotubes in comparison with their corresponding self-assembled ones at 298 (c) and 350 K (d). The color code is identical to that mentioned above.

amino acids with cyclic side chains recently investigated.[20,21] Accordingly, Ac_5c is expected to adapt its folded conformation within the targeted position more easily than the corresponding analogue with a cyclopropane ring. Three Ac_5c-single mutations were considered in this work for each β-helix building block, which were selected based on our previous study (see below).[19] The mutated positions for the 1krr and 1hv9 fragments are displayed in Table 1.

The results presented in this manuscript demonstrate the promising utility of the conformationally restricted amino acids as key pieces to bias the conformational preferences of naturally occurring building blocks. In all cases, we observe favorable formation of coherently organized nanostructures when Ac_5c is introduced in selected positions of the β-helical building block, independently of the conditions studied and the protein segment chosen for the experiments. Thus, nanotubes built by the

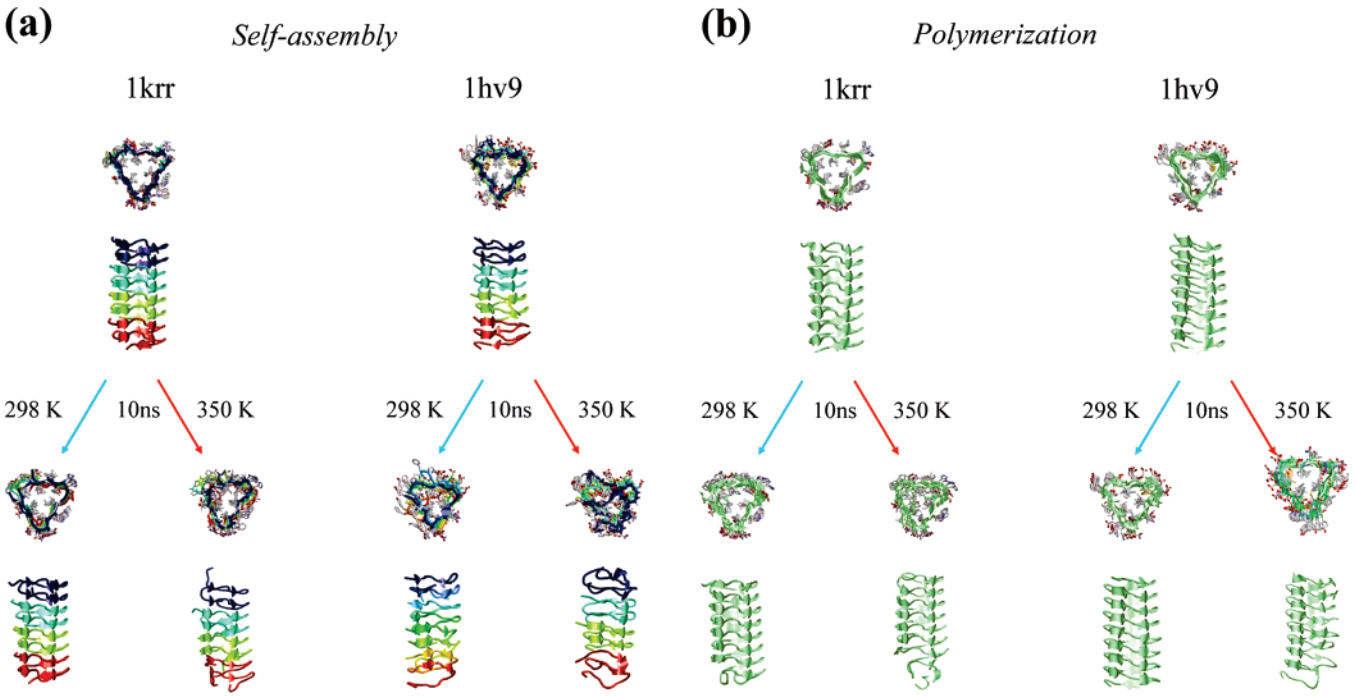

Figure 3. Structure of self-assembled (a) and polymerized (b) nantubes obtained from both 1krr and 1hv9 at the beginning and after 10 ns of MD simulation. In all cases the arrows pointing to the left and right of the starting structures precede the organization sustained at 298 and 350 K, respectively. Note that for the assembled structures each building block is highlighted with different color.

assembly of the 1krr motifs get extra stabilization when Gly 149 is substituted by Ac_5c. Analogous results are obtained when Ac_5c replaces Asp at the position 306 of 1hv9. On the other hand, the promotion of polymerization as compared to self-assembly always increases the thermal stability of the constructs, even when the assembly is not favored as in 1hv9.

Methods

Computational Details. MD simulations were performed using the NAMD program.[40] Each simulated system was placed in the center of an orthorhombic simulation box filled with explicit water molecules, which were represented using the TIP3 model.[41] Positively charged sodium atoms were added to the simulation box in the required amount to reach electric neutrality (all considered building blocks had negative net charge at neutral pH). All atoms of both building blocks and the nanotubes were considered explicitly. The details for each simulated system are provided in Table 2.

The energy was calculated using the AMBER force-field,[42,43] with the required parameters taken from the AMBER libraries for all of the residues with the exception of Ac_5c. A recently developed parametrization[27] that is fully consistent with AMBER parameters was used for this conformationally constrained residue. Atom pair distance cutoffs were applied at 14.0 Å to compute the van der Waals interactions. The electrostatic interactions were computed using the non-truncated electrostatic potential with Ewald summations.[44] The real space term was determined by the van der Waals cut off (14.0 Å), whereas the reciprocal term was estimated by interpolation of the effective charge into a charges mesh with a grid thickness of 5 points per volume unit, i.e., particle-mesh Ewald (PME) method.[44] Bond lengths were constrained using the *SHAKE* algorithm,[45] with a numerical integration step of 2 fs.

Before the production series, the thermodynamic variables of the system were equilibrated. The energy of each system was initially minimized to relax conformational and structural tensions using the conjugate gradient method for at least 5×10^3 steps; that is, the system was subjected to minimization until the difference in energy was less than a threshold of 10^{-6} kcal/mol or the norm of the gradient for two successive steps in the minimization was less than 0.1 kcal/mol·Å. Next, different consecutive rounds of short MD runs were performed in order to equilibrate the density, temperature, and pressure. First, solvent and charged sodium atoms were thermally relaxed by three consecutives runs, while the protein parts were kept frozen. Then, 0.5 ns of NVT−MD at 500 K were used to homogeneously distribute the solvent and ions in the box. Second, 0.5 ns of isothermal and 0.5 ns isobaric relaxation were run. Finally, all of the atoms of the system were submitted to 0.15 ns of steady heating until the target temperature was reached (298 K), 0.25 ns of NVT-MD at 298 K (thermal equilibration) followed by 0.5 ns of density relaxation (NPT-MD). Both temperature and pressure were controlled by the weak coupling method, the Berendsen thermo-barostat,[46] using a time constant for heat bath coupling and a pressure relaxation time of 1 ps. The end of the density relaxation simulation was the starting point of the molecular simulations presented in this work. All of the building block systems were simulated at 298 K and constant pressure of 1 atm. On the other hand, all of the nanotube systems, both self-assembled and covalently linked models, were simulated using the aforementioned conditions to assess their stability at physiological conditions and at higher temperature to partially study their kinetic stability. Thus, in those simulations, the end of NPT relaxation was used as starting point for an NVT simulation at 350 K (more than 50 degrees over standard conditions). The coordinates of all the production runs, which were 10 ns long, were saved every 500 steps (1 ps intervals) for subsequent analysis.

Structural Analyses. The conformational stability and conservation of the nanostructures was measured by calculating (i) the evolution of the backbone root-mean-square deviation (RMSD) through the simulation relative to the initial structure; and (ii) the root-mean-square fluctuation (RMSF) of individual residues averaged over the whole simulation. Both RMSD and RMSF were computed with respect to the backbone atoms ($-N-C^{\alpha}-C-$). The distribution of the backbone dihedral angles φ,ψ was used to show the mobility of the loop regions. The conformation of a given residue is more restrained when the φ,ψ distribution is narrower.

Results and Discussion

Self-Assembled versus Polymerized Nanotubes Derived from Wild-Type 1krr and 1hv9. The overall stability of the self-assembled and polymerized nanotubes of 1krr and 1hv9 was measured by computing the backbone RMSD with respect to the initial structure. Analysis of the RMSDs for simulations performed at 298 K, which are displayed in Figure 2a, indicates that the self-assembled structure of 1krr is very stable (average RMSD = 1.43 ± 0.12 Å), whereas the self-assembled construct of 1hv9 exhibits significant conformational distortions that lead to an increase of the RMSD beyond 2 Å after 1 ns of simulation (average RMSD = 2.18 ± 0.21 Å). Figure 3a compares the two self-assembled structures following 10 ns of simulation, whereas Figure 2c plots the RMSF of these two systems. The low stability of the 1hv9 structure is mainly due to the distortions of the loop regions, especially those formed by segments 304−306 and 321−323. In contrast, no significant fluctuation was found for the self-assembled structure of 1krr after 10 ns. Although no qualitative change is detected when these results are compared with those derived from simulations at 350 K (Figure 2b), self-assembled structures show significant sensitivity toward thermal strain. Thus, the self-assembled structure of 1krr exhibits much higher structural fluctuations at 350 K than at 298 K, even though the core of the assembly remains stable in both cases. Inspection to the RMSF clearly shows that the main distortions are located at the building blocks of the assembly edges, suggesting that this greater flexibility might mostly be a reflection of the finite size of the system. On the other hand, the self-assembled construct based on the 1hv92 building block exhibits the same behavior as previously seen at 298 K. However, at 350 K, the destabilization occurs in a much shorter time lapse (the RMSD gets to 2.5 Å even before reaching 1 ns).

Inspection of the RMSF (Figure 2d) demonstrates that the reduction of nano-organization is homogenously extended to all of the building blocks, analogous to what was seen at 298 K. Therefore, both simulated conditions show the same behavior for the studied assembly cases, with the temperature only enhancing the differences in the kinetic stability among them.

Moreover, these results are in excellent agreement with our previous report,[19] even though different MD conditions were used. Previous simulations were performed with the CHARMM22 force-field using a simulation box of dimensions 50 × 50 × 70 Å with NVT conditions at higher temperature (330 K), whereas the present work was carried out with AMBER force-field[42,43] using an initial box size of 80 × 80 × 110 Å and the density was previously relaxed at 298 K and 1 atm (NPT conditions), whereas 350 K simulations were run in parallel. Hence, it can be concluded that the predictions do not depend on the force-field or on the simulation conditions.

The polymerized nanotubes of 1krr and 1hv9 were constructed by linking covalently the corresponding building blocks. To successfully link these polymeric nanostructures, the covalent linkage of several identical building blocks should guarantee the formation of the desired fold. To provide a homogeneous and regular β-helix fold, a Gly residue, which is not expected to alter the chemical nature of the nanoconstruct due to the lack of side chain, was used. Figure 1b shows the position of the Gly linker between two consecutive 1krr building blocks. In contrast, no linker was needed for the polymerized nanotube of 1hv9, as a regular β-helix arrangement was obtained when the building blocks are linked directly. This structural difference between the nanoconstructs formed by 1krr and 1hv9 was found to be crucial for understanding the stabilities of both self-assembled and polymerized tubes (see below).

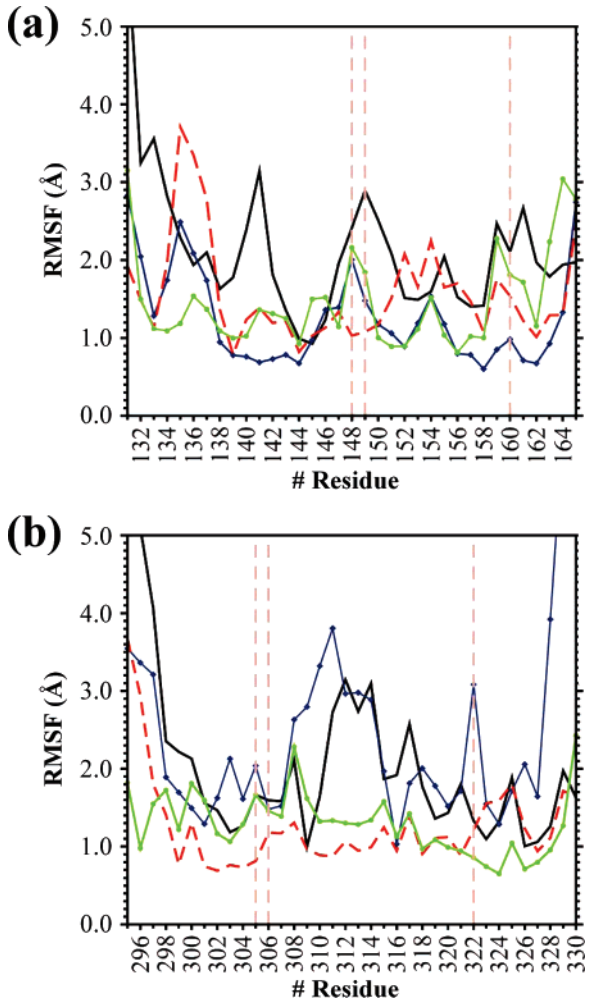

Figure 4. Comparison of the RMSF for the wild type and mutated building blocks. (a) Building blocks based on 1krr: wild type (black line), P148Ac$_5$c (blue line), G149Ac$_5$c (red line), and A160Ac$_5$c (green line). (b) Building blocks based on 1hv9: wild type (black line), D305Ac$_5$c (blue line), D306Ac$_5$c (red line), and A322Ac$_5$c (green line). Gray dashed lines indicate the position of the substitutions.

The evolution of the RMSDs along the simulations for the polymerized nanotubes is included in Figure 2, panels a and b (simulations at 298 and 350 K). The structures obtained at the end of each trajectory are displayed in Figure 3b. Finally, Figures 2c and Figures 2d compare the residue-based fluctuation of the polymerized structures with their corresponding self-assembled ones, at 298K and 350K, respectively. For both 1krr and 1hv9, the polymerized structures are considerably more stable than the self-assembled ones, even though the most significant improvement was obtained for the construct derived from the 1hv9 building block. The average RMSDs are 0.98 ± 0.20 and 0.98 ± 0.13 Å for the tubes formed by polymerizing the 1krr and 1hv9, respectively, showing a reduction of about and 1.2 Å with respect to the self-assembled analogues. The behavior exhibited by both the polymerized and the self-assembled tubes at 350 K is qualitatively analogous to that previously described at 298 K. However, in all cases, the structural fluctuations increase with the temperature. Figure 2d illustrates such behavior, as can be observed by the homogeneous increment of the structural fluctuations along all of the studied sequences when the temperature is raised.

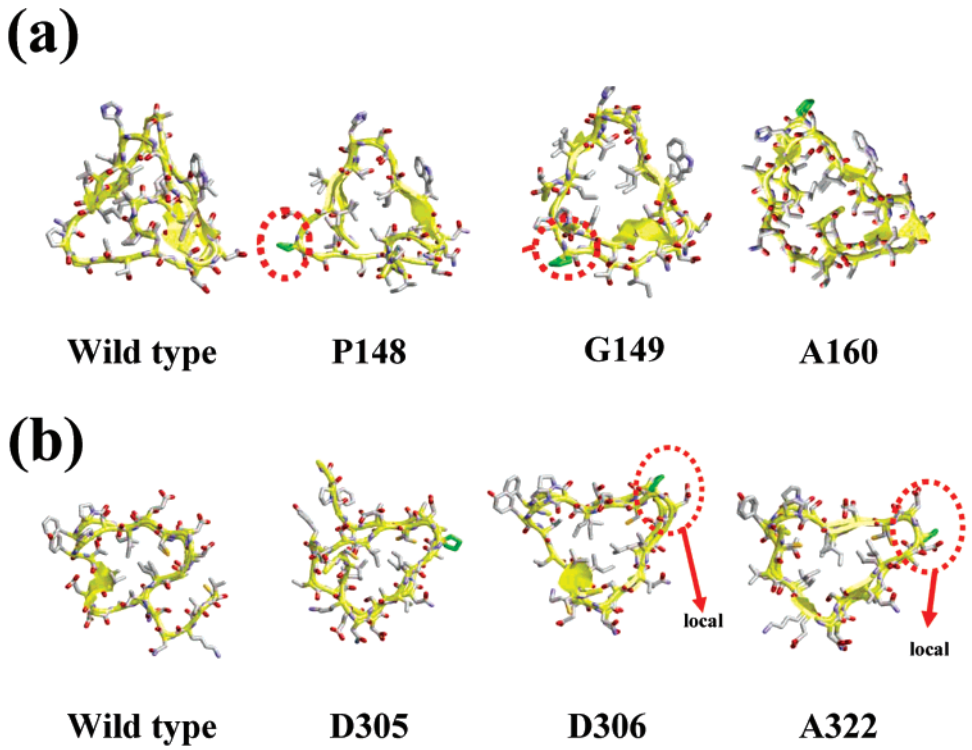

Figure 5. Structure of the wild type and mutated building blocks of 1krr (a) and 1hv9 (b) after 10 ns of MD simulation. The hydrogen atoms have been omitted for clarity and the backbone has been represented by solid shapes (arrows indicate sheet conformation). Circled zones correspond to explicit structural effects that are highlighted in the text.

On the other hand, a detailed comparison of panels a and b in Figure 2 illustrates how covalent linkages between building blocks reduce the unfolding velocity; that is, polymerization provides not only thermal stabilization but also enhances the kinetic stability of the nanoconstructs. Although self-assembled models rapidly lose global organization, those that were covalently linked show similar behavior to that exhibited at 298 K (Figure 3b).

A detailed analysis of the snapshots recorded during the simulation allows explaining the differences found between the nanostructures formed by these two β-helical motifs. As mentioned above, no linker was required to join two consecutive building blocks of 1hv9 indicating that the distance between the end of a repetitive unit and the beginning of the next one is close to that typically found for a chemical bond. This distance, which is excessively short for self-assembling, together with the low inherent conformational stability of the 1hv9 building block, precludes the stabilization of the self-assembled nanoconstruct and induces the unfolding of the loop regions. On the other hand, a larger distance between consecutive building blocks was obtained for 1krr. This distance was suitable for the stabilization of the tube formed by the self-assembled building blocks since optimum nonbonding interactions were obtained between successive repeating units. Finally, the behavior of polymerized nanoconstructs can be straightforwardly explained: the stability of regular and homogeneous conformations increases with the size of the chain.

Overall these results allow us to conclude that the stability of the nanotubes depends on how efficient is the match between consecutive building blocks. Homogeneous β-helix folds can be obtained by forming stable assemblies of building blocks aligned in a complementary (self-assembled) manner or by introducing suitable linkers to retain the backbone hydrogen bonds and the electrostatic interaction in the β-sheet and loop regions.

Stability of Building Block Mutants of 1krr and 1hv9. Three positions of 1krr and 1hv9 were selected as suitable candidates for substitution by Ac_5c according to the following criteria: (i) the residues are located in the loop regions, which display higher mobility than the β sheets and present a turn-conformation similar to that preferred by Ac_5c; (ii) the side chain of the residues is outward-pointing avoiding unfavorable steric interactions between the cyclopentane group of the Ac_5c substitution and the side chains of the inward-pointing residues; and (iii) the charged side chain of the Asp-305 and Asp-306 residues produces electrostatic repulsions in the loop regions of 1hv9. Thus, targeting flexible and electrostatically disfavored loop regions should have direct impact on the structural stability of the nanoconstructs.

For the 1krr building block, the Pro, Gly, and Ala residues at positions 148, 149, and 160 are substituted by Ac_5c one at a time (Table 1), with the three corresponding mutants denoted P148Ac_5c, G149Ac_5c, and A160Ac_5c, respectively. The single mutations performed on the 1hv9 building block at Asp-305, Asp-306, and Ala-322 were denoted D305Ac_5c, D306Ac_5c, and A322Ac_5c, respectively. Figure 4 compares the RMSF of the wild type building blocks with the corresponding mutants, and Figure 5 displays for each case the structure obtained after 10 ns of MD simulation. As can be seen, for the 1krr mutants, the highest local improvement was obtained for G149, the averaged RMS of residue 149 decreasing by about 2 Å. Thus, the substitution of a flexible Gly residue by an Ac_5c, which is constrained to adopt turn conformations, stabilizes the bend architecture of the loop by reducing its mobility. This is reflected in Figure 6a, which shows the Ramachandran plots of the substituted positions and the adjacent residues. As can be seen, the conformations of the Pro-148 and Val-150 residues are significantly more restrained in the mutant than in the wild type.

The P148Ac_5c and A160Ac_5c mutants also display a stabilization of the substituted position, although this local improve-

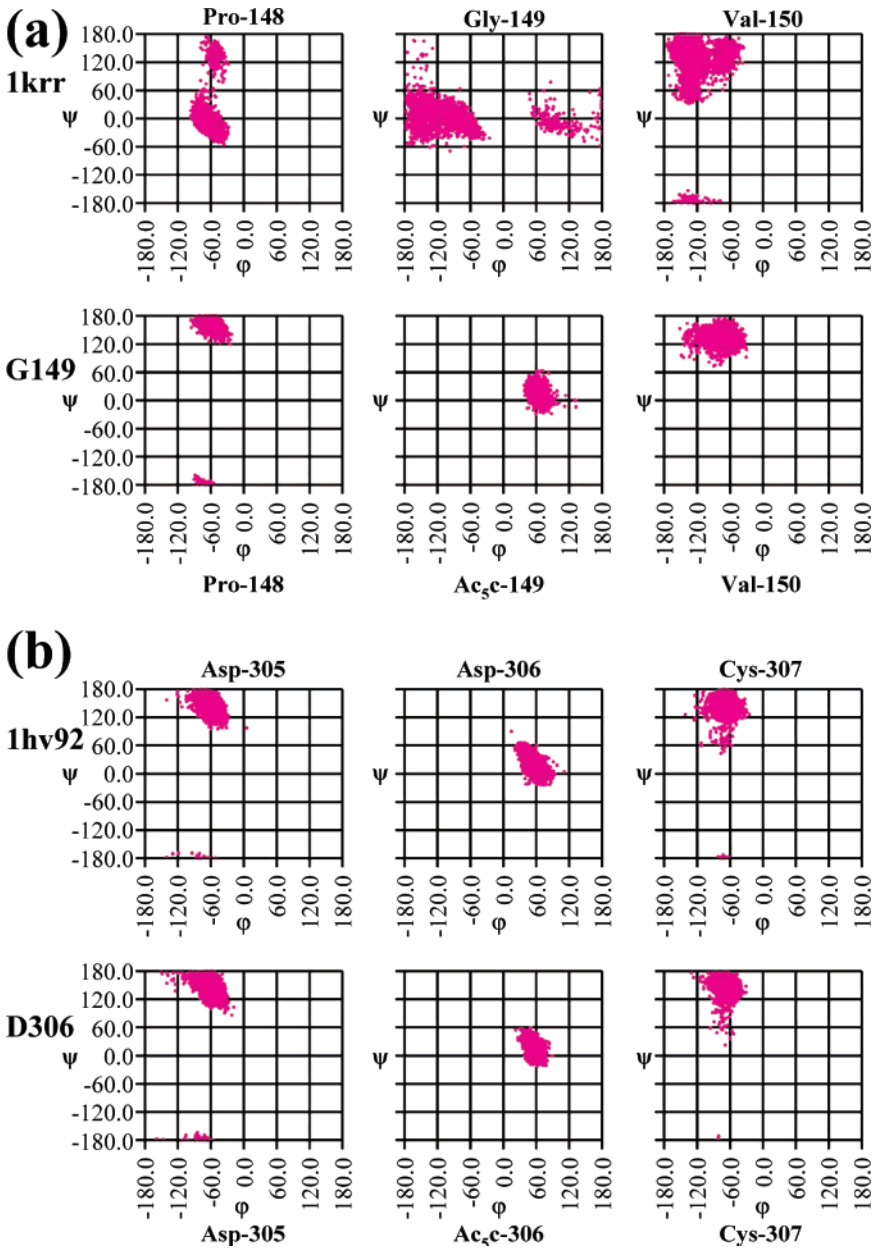

Figure 6. Comparison of the backbone torsion angle (φ, ψ) distributions for the more significant building blocks. The Ramachandran plots correspond to the targeted position and its adjacent residues in (a) 1krr wild type and G149Ac$_5$c mutant and (b) 1hv9 wild type and D306Ac$_5$c mutant.

ment was smaller than 0.5 Å (Figure 4a). In the case of P148Ac$_5$c, this is an expected result. Since Pro also prefers turn conformations,[47] this substitution is less important than that of G149Ac$_5$c. Regarding A160Ac$_5$c, the snapshot recorded at the end of the simulations (Figure 5a) reveals a significant distortion in the turn at positions 148−150. This segment is located between both N- and C-termini edges, implying that it is susceptible to undergo conformational changes when those edges start fraying. Figure 5a also evidence the reorganization of the turn between residues 159−161, which involves the substituted position. Thus, in A160Ac$_5$c, the conformational rigidity of this loop is enhanced inducing a global chain effect that causes the edges to collapse. In the wild type case, the loop spontaneously evolved toward an alternative organization that favors the preservation of the β−helix motif (Figure 5a). In summary, the flexibility of the loop containing Ala-160 is crucial for the global organization of the building block.

Results for the wild type building block of 1hv9 and its three mutants are displayed in Figures 4b and 5b. As can be seen, substitution at Asp-305 does not provide either local or global improvement. The structural distortion is significant and similar for both the wild type and the D305Ac$_5$c mutant, with the β-helix disrupted in both cases. In contrast, a notable structural stability is displayed by the D306Ac$_5$c mutant. In this case, the RMSF is considerably smaller not only at the substitution site but also at all other positions. Thus, the initial β-helix conformation is retained without apparent distortions after 10 ns of MD simulation. Inspection of the Ramachandran plots of the substituted position and the adjacent residues, displayed in Figure 6b, reveals a significant resemblance between the wild type and the D306Ac$_5$c mutant. Even though the substitution at position Asp-306 by Ac$_5$c eliminates the electrostatic repulsion with Asp-305, the backbone constraints associated with the Ac$_5$c residue have a significantly smaller effect in the fluctuations at the loop than at the other positions. As a consequence, a substantial global stabilization of the building block is obtained. Finally, the A322Ac$_5$c mutant shows accept-

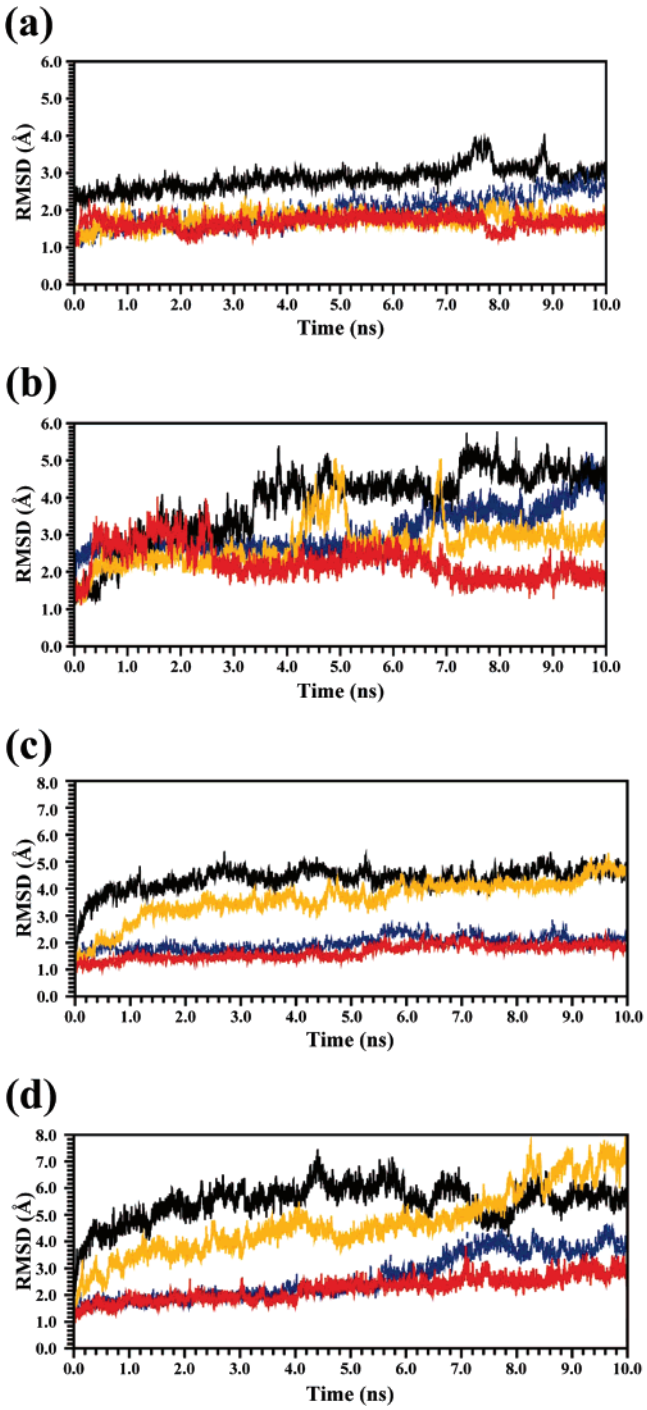

Figure 7. Evolution of the backbone RMSD of the simulated nantube models based upon both wild type sequences and mutants with respect to the initial structures. In the plot are compared assemblies and polymerized structures for each case. For 1krr based nanotubes: wild type self-assembled nanotube (black line), wild type polymerized nantube (blue line), G149Ac$_5$c self-assembled nanotube (orange line) and G149Ac$_5$c polymerized nantube (red line) simulated at (a) 298 and (b) 350 K. For 1hv9 based nanotubes: wild type self-assembled nanotube (black line), wild type polymerized nantube (blue line), D306Ac$_5$c self-assembled nanotube (orange line) and D306Ac$_5$c polymerized nantube (red line) simulated at (c) 298 and (d) 350 K.

able local and global stabilization, which is a consequence of the restrictions imposed by the Ac$_5$c on the backbone conformation.

Stability of the Self-Assembled and Polymerized Nanotubular Mutants of 1krr and 1hv9. G149Ac$_5$c and D306Ac$_5$c were selected as building blocks for self-assembled and polymerized nanotubes. These two mutants provided the largest local and global stabilization for the β-helix motifs derived from 1krr and 1hv9, respectively. The strategy used to build the structures of both self-assembled and polymerized nanotubular mutants was identical to that described above for the wild-type nanoconstructs. The polymerized nanotube of G149Ac$_5$c only formed a homogeneous β-helix when a Gly was introduced as linker residue. Figure 7 compares the evolution of the RMSD calculated for nanotubes of the mutated building blocks with those obtained using wild-type repeats, whereas Figure 8 compares the RMSF. In Figure 7, the simulations performed at 350 K are also included, whereas Figure 8 only depicts the RMSF at 298 K (see text below).

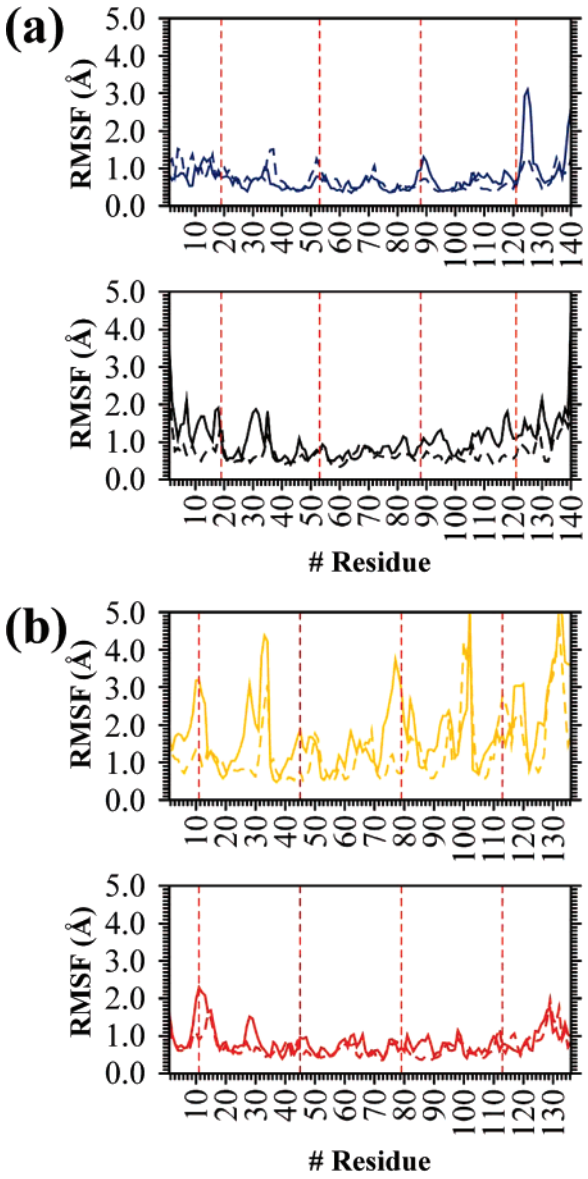

Figure 8. Comparison of RMSF values for the wild type and mutated sequences in both self-assembled (top plots) and polymerized (bottom plots) nanotubes, simulated at 298 K. (a) Nanotubes based on 1krr: On the top, the self-assembled wild type (blue line) and the G149Ac$_5$c (blue-dashed line) building blocks; on the bottom, the polymerized wild type (black line) and G149Ac$_5$c (black-dashed line) building blocks. (b) Nanotubes based on 1hv9: On the top, the self-assembled wild type (orange line) and D306Ac$_5$c (orange-dashed line) building blocks; on the bottom the polymerized wild type (red line) and D306Ac$_5$c (red-dashed line) building blocks.

As can be seen, the RMSD of the G149Ac$_5$c self-assembled system is considerably smaller than its corresponding wild type

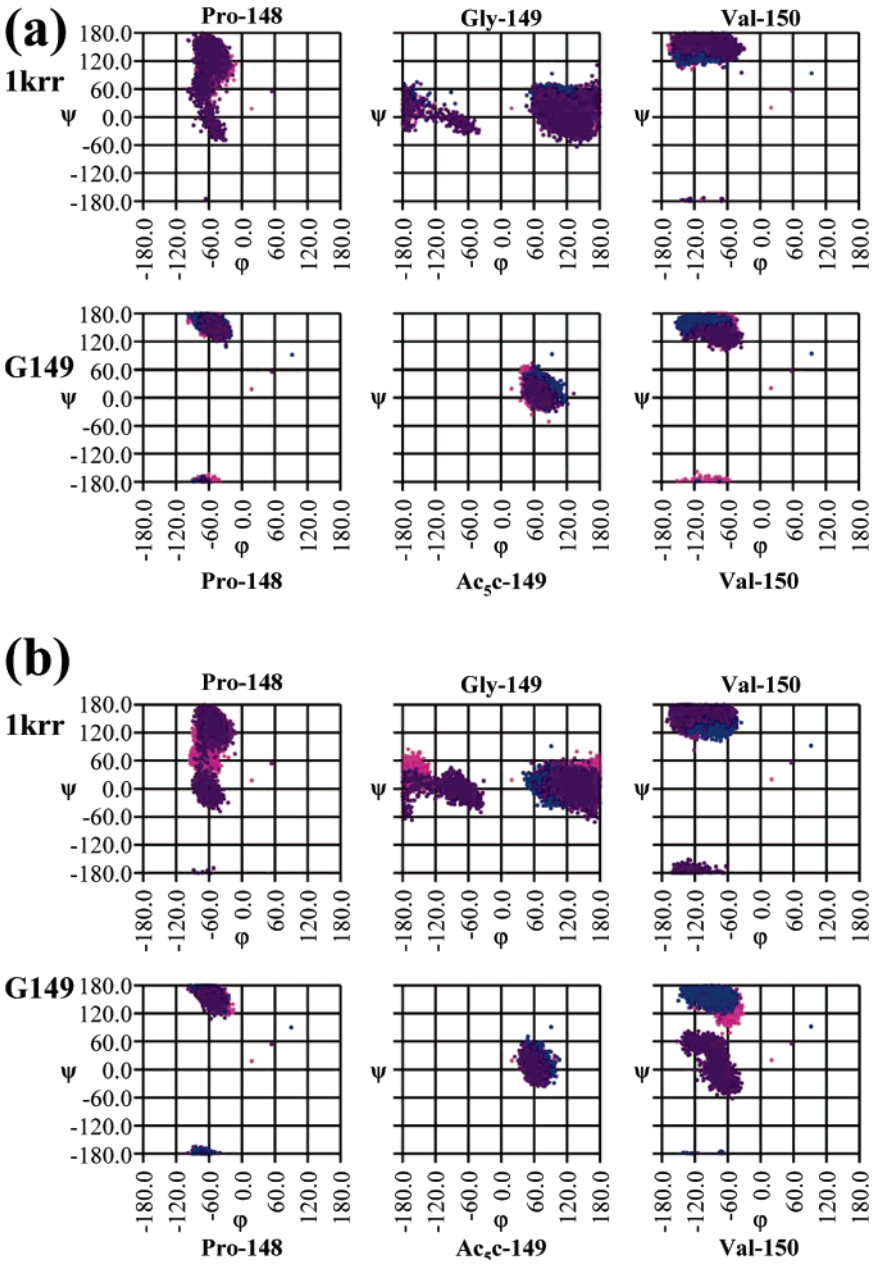

Figure 9. Comparison of the backbone torsion angle (φ, ψ) distributions of the targeted segments for the nanotubes constructed with the 1krr building block simulated at 298 K. The Ramachandran plots correspond to the mutated position and its adjacent residues in the self-assembled (a) and polymerized (b) nanotubes derived from the wild type and G149Ac$_5$c building blocks. Different colors have been used for each building block.

system. At 298 K, the backbone RMSD of the self-assembled G149Ac$_5$c remains close to 1 Å for the whole simulation indicating that the stability of this self-assembled organization is remarkably high. No significant difference was found in the RMSF and Ramachandram plots of all of the 1krr based tubes when the temperature is raised to 350 K. Thus, further results related to the tubes' ultra-structure will only be described for the simulations performed at 298 K (detailed analysis of simulations performed at 350 K is provided in the Supporting Information).

The aforementioned G149Ac$_5$c behavior clearly demonstrates that the substitution of Gly-149 by Ac$_5$c not only reduces the flexibility of the building block but also enhances its ability to retain the assembled structure constructed using the mutated subunits. The latter feature is clearly evidenced by the Ramachandran plots displayed in Figure 9a, which reflect not only the low mobility of the whole mutated loops but also the remarkable conformational similarity among the four Ac$_5$c residues contained in the different subunits of the self-assembled G149Ac$_5$c. This result is particularly important since, although self-assembled nanotubes using 1krr repeats present an intrinsic stability, it can be significantly increased by restricting the conformational freedom at a specific position within the most mobile loop.

On the other hand, Figure 7a suggests a small stabilization when this mutation is introduced in the polymerized tubes, even though the RMSFs are very low and similar to the G149Ac$_5$c and 1krr polymerized systems. Indeed, the Ramachandran plots displayed in Figure 9b indicate that the conformation is more regular for the mutated tube than for the wild-type one. As mentioned above, introduction of Ac5c in position 149 reduces the conformational freedom of the segment enhancing the stability of the conformational motif. Hence, introduction of conformationally restrained residues at suitable positions appears

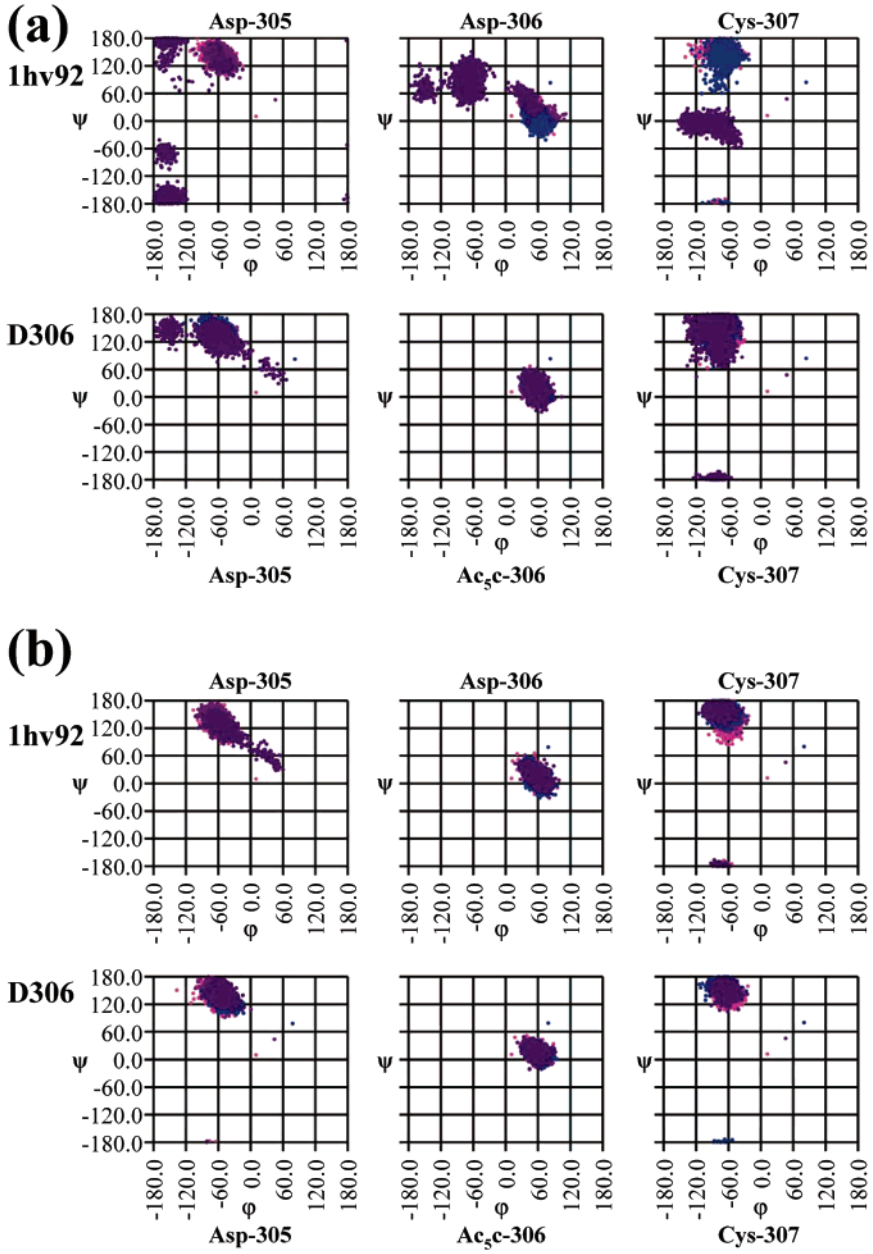

Figure 10. Comparison of the backbone torsion angle (φ, ψ) distributions of the targeted segments for the nanotubes constructed with the 1hv9 building block simulated at 298 K. The Ramachandran plots correspond to the mutated position and its adjacent residues in the self-assembled (a) and polymerized (b) nanotubes derived from the wild type and D306Ac_5c building blocks. Different colors have been used for each building block.

a good strategy to stabilize not only the self-assembled nanoconstructs but also polymerized ones. Comparison of the self-assembled and polymerized nanotubes of G149Ac_5c reveals that both the RMSD and RMSF are very similar for the two systems. Furthermore, the conformations of the Ac_5c and its neighboring residues do not depend on the self-assembled or polymerized nature of the nanotube, being almost identical in both cases. Thus overall these results allow us to conclude that G149Ac_5c is a potentially good mutant of 1krr.

Comparison of the self-assembled and polymerized nanostructures derived from D306Ac_5c with those constructed using the 1hv9 wild type building block is provided in Figure 7, panels c and d, at two different temperatures. Once again, the increment of temperature does not lead to meaningful differences with respect to the simulations performed at 298 K. In order to reduce the background noise introduced by increasing thermal vibrations, ultra-structural details will be provided for the 298 K simulations.

Figure 8b shows the RMSF for all of the 1hv9 based nanotubes studied at 298 K. As can be seen, substitution in the self-assembled tube does not produce any significant improvement. Thus, the RMSD of the D306Ac_5c and 1hv9 self-assembled tubes are very similar after 10 ns of MD simulation. Indeed, inspection to the RMSF values reveals that the mutation at the Asp-306 produces a significant fraying at the C-terminal region of all of the interacting subunits, even though an improvement is clearly observed not only at the substituted position but also at the residues located at the N-terminal and central regions. The reduced conformational flexibility of the mutated loop is illustrated in Figure 10a, which compares the Ramachandran plots of residues 305, 306 and 307 contained in

the four self-assembled subunits. These results indicate that although electrostatic repulsions were removed in the mutated building block, they appear again when the Asp-305 residues of the stacked D306Ac_5c units interact.

Finally, inspection of the RMSD (Figure 7c), RSMF (Figure 8b) and Ramachandran plots of the residues contained in the mutated loop (Figure 10b) of the D306Ac_5c and 1hv9 polymerized tubes shows that mutation by Ac_5c does not produce any relevant variation in the stability of the nanoconstruct. This is because the stability of the polymerized nanostructure constructed using the 1hv9 wild type sequence is very significant. Thus, the unfavorable effects associated with both the conformational flexibility of the loops and the electrostatic repulsions between neighboring Asp are minimized when the building blocks are covalently linked, the influence of the mutation by itself being almost negligible.

Conclusions

The present simulations confirm the intrinsic stability of self-assembled 1krr, which should be attributed to the stabilizing nonbonded interactions of the complementary arrangement of the building blocks. On the other hand, the high stability of the polymerized nanotubes constructed by linking the building blocks through covalent bonds indicates that the main structural principles of polymer chemistry and physics are valid for repeating units made of relatively large fragments of proteins. Thus, polymerization should be considered as a good alternative to self-assembling for the construction of stable nanotubes, especially for 1hv9 building block.

Analysis of the mutated building blocks provides some conclusions with respect to the substitution by the synthetic residue. For the 1krr, the substitution of Gly-149 by Ac_5c has reduced significantly the conformational mobility not only at the mutated position but also of the adjacent positions. On the other hand, for 1hv9 the substitution of Asp-306 by Ac_5c induced a remarkable structural stability, which has been attributed to the elimination of unfavorable electrostatic interactions.

The simulation of the self-assembled and polymerized nanotubes constructed using G149Ac_5c and D306Ac_5c building blocks allow us to derive the following conclusions. First, the G149Ac_5c is a promising mutant of 1krr as revealed by both the significant stabilization found for the self-assembled system and the results obtained for the polymerized tube. Second, the introduction of residues with restrained conformations at strategic positions within the more flexible regions of the β-helix is a good strategy to improve the stability of the nanotubes. Finally, the stabilization induced in a building block by the substitution of a given residue does not guarantee that the same effect will occur in the corresponding nanostructure.

Acknowledgment. Computer resources were generously provided by the Barcelona Supercomputer Center (BSC) and, partially, by Centre de Supercomputació de Catalunya (CESCA) for computational resources. We also acknowledge the National Cancer Institute for partial allocation of computing time and staff support at the Advanced Biomedical Computing Center of the Frederick Cancer Research and Development Center. Classic calculations were partially formed by utilizing the high-performance computational capabilities of the Biowulf PC/Linux cluster at the National Institutes of Health, Bethesda, Md (http://biowulf.nih.gov). D.Z. thanks financial support from the Ramon y Cajal program of the Spanish "Ministerio de Educación y Ciencia" (MEC). F.R.-R. also thanks the Spanish MEC for financial support. This project has been funded in whole or in part with Federal funds from the National Cancer Institute, National Institutes of Health, under Contract No. N01-CO-12400. The content of this publication does not necessarily reflect the view of the policies of the Department of Health and Human Services, nor does mention of trade names, commercial products, or organization imply endorsement by the U.S. Government. This research was supported [in part] by the Intramural Research Program of the NIH, National Cancer Institute, Center for Cancer Research.

Supporting Information Available. Averaged root-mean-square fluctuations for the wild type and mutated sequences in both self-assembled and polymerized nanotubes simulated at 350 K. Ramachandran plots for the nanotubes constructed with 1krr and 1hv9 building blocks simulated at 350 K. This information is available free of charge via the Internet at http://pubs.acs.org.

References and Notes

(1) Ferrari, M. *Nat. Rev. Cancer* **2005**, *5*, 161.
(2) Ferrari, M. *Curr. Opin. Chem. Biol.* **2005**, *9*, 343.
(3) Alemán, C.; Zanuy, D.; Jiménez, A. I.; Cativiela, C.; Haspel, N.; Zheng, J.; Wolfson, H; Nussinov, R. *Phys. Biol.* **2006**, *3*, S54.
(4) Claussen, R. C.; Rabatic, B. M.; Stupp, S. I. *J. Am. Chem. Soc.* **2003**, *125*, 12680.
(5) Percec, V.; Dulcey, A. E.; Balagurusamy, V. S.; Miura, Y.; Smidrkal, J.; Peterca, M.; Nummelin, S.; Edlund, U.; Hudson, S. D.; Heiney, P. A.; Hu, D. A.; Magonov, S. N.; Vinogradov, S. A. *Nature* **2004**, *430*, 764.
(6) Rajagopal, K.; Schneider, J. P. *Curr. Opin. Struct. Biol.* **2004**, *14*, 480.
(7) Valery, C.; Paternostre, M.; Robert, B.; Gulik-Krzywicki, T.; Narayanan, T.; Dedieu, J. C.; Keller, G.; Torres, M. L.; Cherif-Cheikh, R.; Calvo, P.; Artzner, F. *Proc. Natl. Acad. Sci. U.S.A.* **2003**, *100*, 10258.
(8) Rathore, O.; Sogah, D. Y. *J. Am. Chem. Soc.* **2001**, *123*, 5231.
(9) Vauthey, S.; Santoso, S.; Gong, H.; Watson, N.; Zhang, S. *Proc. Natl. Acad. Sci. U.S.A.* **2002**, *99*, 5355.
(10) Yokoi, H.; Kinoshita, T.; Zhang, S. *Proc. Natl. Acad. Sci. U.S.A.* **2005**, *102*, 8414.
(11) Tsai, C.-J.; Maizel, J. V., Jr.; Nussinov, R. *Proc. Natl. Acad. Sci. U.S.A.* **2000**, *97*, 12038.
(12) Tsai, H.-H.; Tsai, C.-J.; Ma, B.; Nussinov, R. *Protein Sci.* **2004**, *13*, 2753.
(13) Liao, S.; Seeman, N. C. *Science* **2004**, *306*, 2072.
(14) Yan, H.; Park, S. H.; Finkelstein, G.; Reif, J. H.; LaBean, T. H. *Science* **2003**, *301*, 1882.
(15) Chworos, A.; Severcan, I.; Koyfman, A. Y.; Weinkam, P.; Oroudjev, E.; Hansma, H. G.; Jaeger, L. *Science* **2004**, *306*, 2068.
(16) Main, E. R. G.; Lowe, A. R.; Mochrie, S. G. J.; Jackson, S. E.; Regan, L. *Curr. Opin. Struct. Biol.* **2005**, *15*, 464.
(17) Kajander, T.; Cortajarena, A. L.; Main, E. R. G.; Mochrie, S. G. J.; Regan, L. *J. Am. Chem. Soc.* **2005**, *127*, 10188.
(18) Main, E. R. G.; Stott, K.; Jackson, S. E.; Regan, L. *Proc. Natl. Acad. Sci. U.S.A.* **2005**, *102*, 5721.
(19) Haspel, N.; Zanuy, D.; Aleman, C.; Wolfson, H.; Nussinov, R. *Structure* **2006**, *14*, 1137.
(20) Zheng, J.; Zanuy, D.; Haspel, N.; Tsai, C.-J.; Alemán, C.; Nussinov, R. *Biochemistry* **2007**, *46*, 1205.
(21) Zanuy, D.; Jiménez, A. I.; Cativiela, C.; Nussinov, R.; Alemán, C. *J. Phys. Chem. B* **2007**, *111*, 3236.
(22) Haspel, N.; Zanuy, D.; Zheng, J.; Alemán, C.; Wolfson, H.; Nussinov, R. *Biophys. J.* **2007**, *93*, 245.
(23) Zanuy, D.; Ma, B.; Nussinov, R. *Biophys. J.* **2003**, *84*, 1884.
(24) Haspel, N.; Zanuy, D.; Ma, B.; Wolfson, H.; Nussinov, R. *J. Mol. Biol.* **2005**, *345*, 1213.
(25) Zanuy, D.; Nussinov, R. *J. Mol. Biol.* **2003**, *329*, 565.
(26) Zanuy, D.; Gunasekaran, K.; Lesk, A. M.; Nussinov, R. *J. Mol. Biol.* **2006**, *358*, 330.
(27) Alemán, C.; Zanuy, D.; Casanovas, J.; Cativiela, C.; Nussinov, R. *J. Phys. Chem. B* **2006**, *110*, 21264.
(28) Cheng, R. P.; Gellman, S. H.; DeGrado, W. F. *Chem. Rev.* **2001**, *101*, 3219.

(29) Xie, J. M.; Schultz P. G. *Curr. Opin. Chem. Biol.* **2005**, *9*, 548.
(30) Pye, V. E.; Tingey, A. P.; Robson, R. L.; Moody, P. C. E. *J. Biol. Chem.* **2004**, *279*, 40729.
(31) Govaerts, C.; Wille, H.; Prusiner, S. B.; Cohen, F. E. *Proc. Natl. Acad. Sci. U.S.A.* **2004**, *101*, 8342.
(32) Kreisberg, J. F.; Betts, S. D.; King, J. *Protein Sci.* **2000**, *9*, 2338.
(33) Adzhubei, A. A.; Sternberg, M. J. E. *J. Mol. Biol.* **1993**, *229*, 472.
(34) Kostrewa, D.; D'Arcy, A.; Takacs, B.; Kamber, M. *J. Mol. Biol.* **2001**, *305*, 279.
(35) Sugantino, M.; Roderick, S. L. *Biochemistry* **2002**, *41*, 2209.
(36) Iverson, T. M.; Alber, B. E.; Kisker, C.; Ferry, J. G.; Rees, D. C. *Biochemistry* **2000**, *39*, 9222.
(37) Jenkins, J.; Mayans, O.; Pickersgill, R. *J. Struct. Biol.* **1998**, *122*, 236.
(38) Toniolo, C.; Crisma, M.; Formaggio, F.; Peggion, C. *Biopolymers (Pept. Sci.)* **2001**, *60*, 396.
(39) Benedetti, E. *Biopolymers (Pept. Sci.)* **1996**, *40*, 3.
(40) Phillips, J. C.; Braun, R.; Wang, W.; Gumbart, J.; Tajkhorshid, E.; Villa, E.; Chipot, C.; Skeel, R. D.; Kale, L.; Schulten, K. *J. Comput. Chem.* **2005**, *26*, 1781.
(41) Jorgensen, W. L.; Chandrasekhar, J.; Madura, J. D.; Impey, R. W.; Klein, M. L. *J. Chem. Phys.* **1983**, *79*, 926.
(42) Wang, J.; Cieplak, P.; Kollman, P. A. *J. Comput. Chem.* **2000**, *21*, 1049.
(43) Cornell, W. D.; Cieplak, P.; Bayly, C. I.; Gould, I. R.; Merz, K. M.; Ferguson, D. M.; Spellmeyer, D. C.; Fox, T.; Caldwell, J. W.; Kollman, P. A. *J. Am. Chem. Soc.* **1995**, *117*, 5179.
(44) Darden, T.; York, D.; Pedersen, L. *J. Chem. Phys.* **1993**, *98*, 10089.
(45) Ryckaert, J. P.; Ciccotti, G.; Berendsen, H. J. C. *J. Comput. Phys.* **1977**, *23*, 327.
(46) Berendsen, H. J. C.; Postma, J. P. M.; van Gunsteren, W. F.; DiNola, A.; Haak, J. R. *J. Chem. Phys.* **1984**, *81*, 3684.
(47) (a) Mac Arthur, M. W.; Thornton, J. M. *J. Mol. Biol.* **1991**, *218*, 397. (b) Gibbs, A. C.; Bjorndahl, T. C.; Hodges, R. S.; Wishart, D. S. *J. Am. Chem. Soc.* **2002**, *124*, 1203. (c) Richardson, J. S.; Richardson, D. C. Principles and patterns of protein conformation. In *Prediction of Protein Structure and the Principles of Protein Conformation*; Fasman, G. D., Ed.; Plenum: New York, 1989; pp 1−98.

BM700561T